SCIENTIFIC REPORTS

OPEN

Anisotropy dependence of the fluctuation spectroscopy in the critical and gaussian regimes in superconducting $NaFe_{1-x}Co_xAs$ single crystals

Received: 25 January 2018
Accepted: 23 May 2018
Published online: 04 June 2018

D. Ahmad[1,2], W. J. Choi[1], D. Sóñora[3], Yoon Seok Oh[2], J. Mosqueira[3], Tuson Park[4] & Yong Seung Kwon[1]

We investigate thermal fluctuations in terms of diamagnetism and magnetotransport in superconducting $NaFe_{1-x}Co_xAs$ single crystals with different doping levels. Results show that in the case of optimal doped and lightly overdoped ($x = 0.03, 0.05$) crystals the analysis in the critical as well as in the Gaussian fluctuation regions is consistent with the Ginzburg-Landau 3D fluctuation theory. However, in the case of strongly overdoped samples ($x \geq 0.07$) the Ullah-Dorsey scaling of the fluctuation induced magnetoconductivity in the critical region confirms that thermal fluctuations exhibit a 3D anisotropic nature only in a narrow temperature region around $T_c(H)$. This is consistent with the fact that in these samples the fluctuation effects in the Gaussian region above T_c may be described by the Lawrence-Doniach approach. Our results indicate that the anisotropy of these materials increases significantly with the doping level.

The phenomenological description of preformed Cooper pairs above T_c as a result of fluctuations of the superconducting order parameter has remained as one of the most important topics in the field of superconductivity. In addition to their intrinsic interest, the analysis of fluctuation effects in the vicinity of the transition temperature T_c also allow to obtain superconducting parameters such as the upper critical field, the coherence length, the anisotropy and the dimensionality. One striking feature of the superconducting fluctuations is their effect on vortex motion which in turn results in a rounding effect near T_c in the magneto-resistance and the magnetization[1–5]. The rounding effect is quantified by the so-called Ginzburg number $G_i = (k_B/4\pi\xi_{ab}(0)\xi_c(0)\Delta c)^2/2$, where Δc is the specific heat jump at T_c, k_B the Boltzmann constant, and $\xi_{ab}(0)$ and $\xi_c(0)$ are the in-plane and c-axis coherence lengths extrapolated to 0 K. G_i in the iron-based superconductors was found to be in between the values corresponding to high T_c and conventional low T_c superconductors[6–8]. For example, in $SmFeAs_{0.85}F_{0.15}$ a value of G_i as large as $\sim 1.6 \times 10^{-2}$ was estimated[6,7], while in Co-doped $BaFe_2As_2$ single crystals G_i is in the range of $\sim 10^{-5}$[8]. The value of G_i in $NaFe_{1-x}Co_xAs$ was estimated to be of the order of 10^{-4} from the $\xi_{ab}(0)$ and $\xi_c(0)$ values obtained below, and from the Δc value in ref.[9]. So far, experimental investigation of the fluctuation effects has been performed through observables such as the specific heat[6,10,11], the magnetization[11–30], the electrical conductivity[7,8,11,21–29] and the microwave conductivity[30]. The fluctuation effects in high T_c superconductors have been well understood in terms of the Lawrence-Doniach (LD) model for layered superconductors[31]. In the case of iron pnictides there's some controversy about the dimensionality of fluctuation effects. For instance, some works reported a two-dimensional (2D) behavior in compounds from the 1111 family like SmFeAsO[7], and from the 111 family like LiFeAs[23,24]. However, some recent reports showed a 3D anisotropic behavior in compounds from the same families[6,16,32].

[1]Department of Emerging Materials Science, DGIST, Daegu, 42988, Republic of Korea. [2]Department of Physics, Ulsan National Institute of Science and Technology, Ulsan, 44919, Republic of Korea. [3]LBTS, Departamento de Física de Partículas, Universidade de Santiago de Compostela, E-15782, Santiago de Compostela, Spain. [4]Creative Research Center for Quantum Materials and Superconductivity, Sungkyunkwan University, Suwon, Republic of Korea. Correspondence and requests for materials should be addressed to Y.S.K. (email: yskwon@dgist.ac.kr)

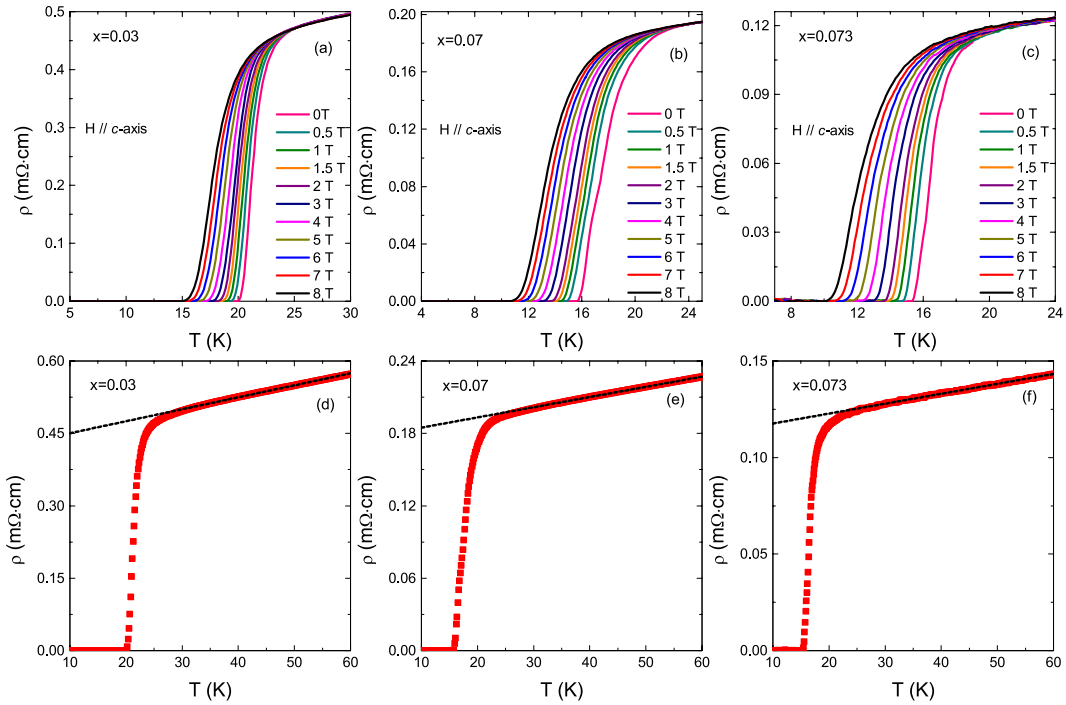

Figure 1. (**a**–**c**) Temperature dependence of resistivity near T_c for $NaFe_{1-x}Co_xAs$ ($x = 0.03, 0.07, 0.073$) crystals under different magnetic fields up to 8 T applied perpendicular to the crystals' *ab*-planes. (**d**–**f**) Example (for $\mu_0 H = 0$ T) of the procedure used to determine the background contribution by a linear fit above 1.5 T_c (lines).

In this paper, we investigate the superconducting fluctuation effects in the magnetization and electrical conductivity of $NaFe_{1-x}Co_xAs$ single crystals with $x = 0.03$, 0.05, 0.07, 0.073, which cover from the optimal doping to the highly overdoped regime. This compound presents a PbClF-type crystal structure, in which Na^+-ions are sandwiched between the FeAs layers[33]. The bulk superconductivity is induced upon Co doping, the maximum T_c occurring for $x = 0.028$[9]. We study both the critical and the Gaussian fluctuation regimes, by using the Ullah and Dorsey scaling and, respectively, the 3DGinzburg-Landau approach and the quasi-2D Lawrence-Doniach model[2,26]. This work extends a previous study of critical fluctuation effects in the magnetization of optimally doped $NaFe_{1-x}Co_xAs$ ($x = 0.03$)[16], and will allow to explore the dependence of the superconducting parameters and of the dimensionality with the doping level.

Results and Discussion

Figure 1(a–c) presents the temperature dependence of the resistivity near T_c under various magnetic fields applied parallel to the crystals' *c*-axis in optimally doped ($x = 0.03$) and overdoped ($x = 0.07$, 0.073) $NaFe_{1-x}Co_xAs$ crystals. In zero applied magnetic field, the critical temperatures for $x = 0.03$, 0.07 and 0.073 are 20.9 K, 16.4 K, and 16.3 K, respectively, as determined from the maximum of $d\rho/dT$. In this representation it may be already appreciated a rounding just above T_c that increases with the applied magnetic field and that may be attributed to superconducting fluctuations. In Fig. 1(d–f) it is presented an example of the normal-state background extraction procedure, that consist in a linear fit above 1.5 T_c, a temperature above which fluctuation effects are expected to be negligible[14,20,26].

We first analyze fluctuation effects in the critical region around the $T_c(H)$ line. In this region, in presence of large magnetic fields the paired quasi-particles are limited to remain in their lowest Landau level and the superconducting fluctuations present a one-dimensional character along the magnetic field direction[2,3]. This lower dimensionality significantly enhances the fluctuation effects in a region bounded by the so-called H-dependent Ginzburg criterion, which for 3D materials may be expressed as[6]

$$\left|\frac{T - T_c(H)}{T_c}\right| \leq \left(\frac{4\pi k_B \mu_0 H}{\Delta c \xi_c(0) \phi_0}\right)^{2/3} \quad (1)$$

where ϕ_0 is the flux quantum and μ_0 the vacuum magnetic permeability. In this region, Ullah and Dorsey (UD) used a self-consistent Hartree approximation to treat the quadratic terms in the Ginzburg-Landau free energy, and obtained an expression for different fluctuation-induced observables. In the case of 3D superconductors, they found that the electrical conductivity follows a scaling behavior that is given by

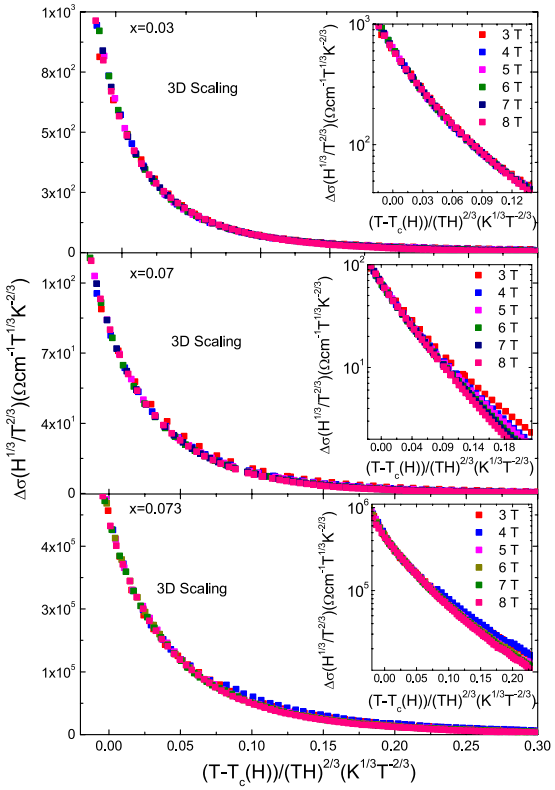

Figure 2. 3D LLL scaling of the fluctuation conductivity for $NaFe_{1-x}Co_xAs$ with $x = 0.03$ (**a**), x = 0.07 (**b**), x = 0.073 (**c**). The Insets show the same data in semi-logarithmic scale.

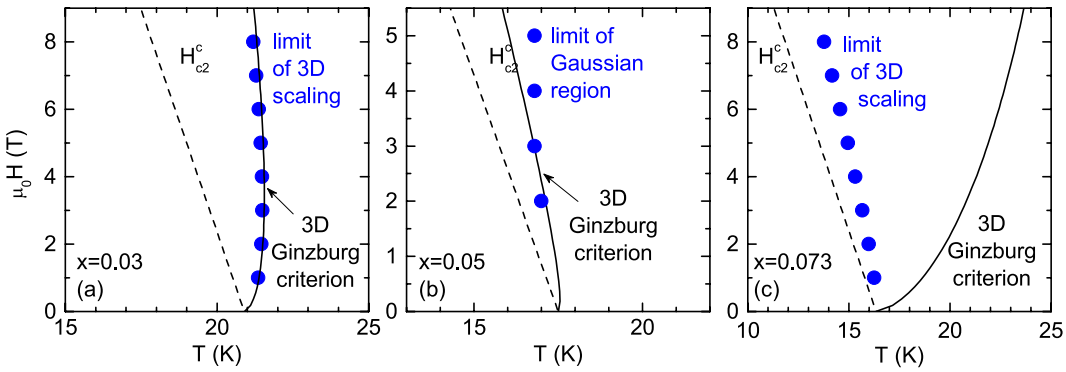

Figure 3. *H-T* phase diagrams of $NaFe_{1-x}Co_xAs$ for $H \perp ab$; (**a**) $x = 0.03$, (**b**) $x = 0.05$, and (**c**) $x = 0.073$, respectively. The corresponding $H_{c2}(T)$ lines were obtained from the superconducting parameters obtained in the analysis. The symbols are the limit of 3D scaling ($x = 0.03, 0.073$) and limit of Gaussian region ($x = 0.05$). The solid lines are the 3D Ginzburg criterion.

$$\Delta\sigma_{3D}^{UD}(T, H) = \left[\frac{T^2}{H}\right]^{2/3} f_{3D}\left[\frac{T - T_c(H)}{(TH)^{2/3}}\right] \tag{2}$$

where f_{3D} is the scaling function. Figure 2 shows the 3D-UD scaling of $\Delta\sigma$ for the optimally doped ($x = 0.03$) and two overdoped ($x = 0.07$ and 0.073) crystals, under different applied fields. The H-dependence of the mean-field critical temperature, $T_c(H)$, is used as a free parameter. The result may be affected by some uncertainty (the difficulties associated to scaling analysis of the electrical conductivity are described in detail in ref.[34]), but the result agrees with the values obtained from a 50% criterion on the normal state resistivity within 2% uncertainty. The insets in Fig. 2 show the same data in semi-logarithmic scale. It is clear from these figures that in the optimally doped crystal the 3D scaling is valid up to higher scaled temperatures than in the $x = 0.07$ and 0.073 crystals. This may also be seen in the *H-T* phase diagrams presented in Fig. 3, where the upper temperature limit of the 3D scaling is compared to the Ginzburg criterion, Eq. (1), as evaluated by using the $\xi_c(0)$ value obtained in the

Value of x	T_c (K)	$\xi_c(0)$ (nm)	$\xi_{ab}(0)$ (nm)	$\mu_0 H_{c2}(0)$ (T)	γ
0.03	20.9	0.8	2.4	55	3
0.05	17.5	1.9	3.3	30	1.75
0.073	16.3	0.23	3.36	29.1	14.6

Table 1. Superconducting parameters of the studied $NaFe_{1-x}Co_xAs$ single crystals.

analysis in the analysis in the Gaussian region (see below), the Δc value for $x = 0.03$ in ref.[9], and the Δc values for overdoped crystals expected from the $\Delta c/T_c$ vs T_c correlation in[35]. In the case of the $x = 0.03$ crystal, the region where the 3D scaling is applicable is in excellent agreement with the prediction. The 3D scaling was also previously observed under similar field amplitudes in the fluctuation-induced magnetic susceptibility of a crystal of the same composition[16], in single crystals of other iron-pnictide families[6,8,12,14,19,20], and also in high-T_c superconductors like optimally-doped $YBa_2Cu_3O_x$[5,36]. In the case of the $x = 0.07$ and 0.073 crystals the 3D-LLL scaling fails before reaching the Ginzburg criterion. This could indicate that the anisotropy increases with the doping level (as previously reported in 122 compounds[18]), to the point that a 3D-2D transition could appear on increasing the temperature above T_c. The analysis in the Gaussian region presented below seems to support this scenario.

From a linear extrapolation to $T = 0$ K of the $T_c(H)$ data obtained in the scalings we obtained that the upper critical fields $H_{c2}(0)$ for the $x = 0.03$, 0.07, and 0.073 crystals were estimated to be 58 T, 38 T and 41 T, respectively. From these values, the Ginzburg-Landau in-plane coherence length amplitudes, $\xi_{ab}(0) = [\phi_0/2\pi\mu_0 H_{c2}(0)]^{1/2}$ resulted to be 2.4 nm, 2.9 nm, and 2.8 nm, respectively. In spite of the uncertainty associated to the extrapolation to $T = 0$ K, these values are in reasonable agreement with the ones listed in Table 1, derived from the subsequent analysis in the Gaussian region (see below).

In order to further investigate the fluctuation effects in the critical region, we measured the temperature dependence of the magnetic moment for the slightly overdoped crystal ($x = 0.05$). These measurements, presented in Fig. 4(a), were performed with magnetic fields up to 5 T perpendicular to the ab layers, under zero-field-cooled (ZFC) and field-cooled (FC) conditions. As it may be seen in this figure, a rounding effect just below T_c (which becomes more prominent upon increasing the applied magnetic field) and a broadening of the reversible region (where the ZFC and FC curves coincide) below T_c, are substantial evidences of the fluctuation effects in the critical region, in agreement with recent results[13,14,16]. In this case the background contribution (which is mainly due to the crystal's normal state) was determined by fitting a curie-like dependence $m_B(T) = a + bT + c/T$ to the as-measured $m(T)_H$ data in the temperature range from 25 K to 45 K (solid lines in Fig. 4(b)). The 3D-UD scaling of the fluctuation magnetization in the critical region is presented in Fig. 5(a). In this case the scaling variables are $[T - T_c(H)]/(TH)^{2/3}$ for the temperature and $M/(TH)^{2/3}$ for the magnetization. We assumed a linear $T_c(H)$ behavior and obtained a good scaling with $T_c = 17.5$ K and $\mu_0 H_{c2}(0) = 30$ T, see Fig. 5(a). These values are consistent with the analysis in the Gaussian region presented below (see Table 1).

In what follows we complement our study with the analysis of fluctuation effects in the Gaussian region well above the $T_c(H)$ line, where the quartic term in the free energy may be neglected. Contrary to the critical region, where the different observables present a relatively smooth temperature dependence, in the Gaussian region they present a divergent behavior on approaching the superconducting transition, and this requires that the superconducting transition width, ΔT_c, is small relative to the T_c value. In particular, it is expected that a possible T_c distribution affects the Gaussian fluctuation effects below a temperature roughly given by $T_{inh} \sim T_c + \Delta T_c$. In the presence of a magnetic field, due to the $T_c(H)$ shift, the region affected by the T_c distribution is displaced to lower temperatures according to $T_{inh} \sim T_c + \Delta T_c - H/[H_{c2}(0)/T_c]$. In the case of the $x = 0.05$ crystal ΔT_c is estimated to be ~1 K from the temperature above T_c at which the low-field magnetic moment (inset in Fig. 5) becomes 10^{-3} times the low-temperature saturation value. By taking into account the $\mu_0 H_{c2}(0)$ value for this sample (30 T), it is expected that a 2 T magnetic field is enough to displace T_{inh} below the own T_c value. In Fig. 5(b) we present the analysis of the fluctuation magnetization in the Gaussian region in terms of the Ginzburg-Landau approach for three-dimensional anisotropic superconductors under finite applied magnetic fields, which may be expressed as[37]

$$M_{fl}^{\parallel}(T, H) = -\frac{K_B T\gamma}{\pi\phi_0\xi_{ab}(0)}\int_0^{\sqrt{c-\varepsilon}} dq\left[\frac{c-\varepsilon}{2h} - \ln\Gamma\left(\frac{\varepsilon + h + q^2}{2h}\right) + \left(\frac{\varepsilon + q^2}{2h}\right)\psi\left(\frac{\varepsilon + h + q^2}{2h}\right) + \ln\Gamma\left(\frac{c + h + q^2}{2h}\right) - \left(\frac{c + q^2}{2h}\right)\psi\left(\frac{c + h + q^2}{2h}\right)\right]. \quad (3)$$

Here Γ and ψ are the gamma and digamma functions, respectively, $\varepsilon = \ln(T/T_c)$ the reduced temperature, $h = \frac{H}{H_{c2}(0)} = H/[\phi_0/2\pi\mu_0\,\xi_{ab}^2(0)]$ the reduced magnetic field, γ the anisotropy factor, and c the total energy cutoff constant, introduced to take into account short-wavelength effects[38]. To compare Eq. (3) with the data we used the T_c and $\mu_0 H_{c2}(0)$ values resulting from the scaling in the critical region, and used for the remaining parameters $\gamma = 1.75$ and $c = 0.35$ (in agreement with the one found in other iron-based superconductors[18,26,27]). A good agreement with the experimental results is obtained, confirming the 3D nature of the $x = 0.05$ crystal. As commented above, the data obtained with magnetic fields below 2 T (not shown) do not follow the Gaussian approach, probably due to a possible T_c distribution. However, it has been also proposed that under these low field amplitudes

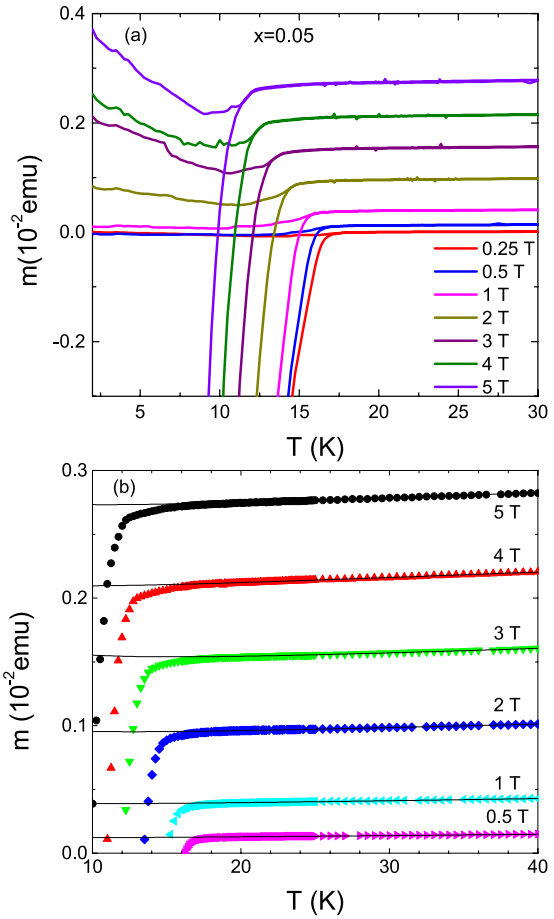

Figure 4. **(a)** Temperature dependence of the magnetic moment of the $NaFe_{1-x}Co_xAs$ ($x = 0.05$) single crystal. These measurements were performed under different magnetic fields applied parallel to c-axis in ZFC and FC modes. (**b**) The background contribution (solid lines) were determined by fitting a Curie-like function above 25 K (where fluctuation effects are expected to be negligible), and up to 40 K.

phase fluctuations may play an important role[15,26]. Another possibility may be that $H_{c2}(T)$ is not linear at these field amplitudes (near T_c), an effect that some attribute to the multiband nature of these compounds[19,39,40]. Just for completeness, we also include as a dashed line the prediction of the 2D-GL approach for $H = 0$ (Eq. (7) in ref.[20] after setting $r = 0$), that strongly overestimates the measured $\Delta M/H$ amplitude. Finally, as it may be seen in Fig. 3(b), the lower temperature limit of applicability of the Gaussian approach is close to the prediction of the H-dependent Ginzburg criterion for the onset of critical fluctuation effects, Eq. (1), as evaluated with the $\xi_c(0)$ value in Table 1, and the Δc value estimated from ref.[35].

The analysis of $\Delta\sigma$ in the Gaussian region for the optimally doped and highly overdoped crystals is presented in Figs. 6 and 7, respectively. In the case of the $x = 0.03$ and 0.073 crystals, the ΔT_c values (obtained from the FWHM of the $d\rho/dT$ curve) are about 1.4 K. Taking into account that for these samples $\mu_0 H^c_{c2}(0) \sim 55$ T and, respectively, ~29 T, according to the above argument it is expected that a 2 T field parallel to the c axis will allow to analyze fluctuation effects down to ~0.6 K and ~0.3 K above T_c, respectively. The optimally doped ($x = 0.03$) crystal is analyzed in terms of a GL approach for 3D anisotropic superconductors that includes an energy cutoff to extend the applicability of the GL approach to high reduced temperatures[26]. In the framework of this approach, that has been successfully applied in iron-based superconductors[20,26,27], the fluctuation-induced conductivity in presence of a magnetic field with an arbitrary orientation is given by

$$\Delta\sigma_{ab} = \frac{e^2}{32\hbar\pi\xi_c(0)}\sqrt{\frac{2}{h}}\int_0^{\sqrt{\frac{c-\varepsilon}{2h}}} dx\left[\psi^1\left(\frac{\varepsilon+h}{2h}+x^2\right)-\psi^1\left(\frac{c+h}{2h}+x^2\right)\right], \tag{4}$$

where $\hbar$ is Planck's constant and e the electron charge. In the absence of applied magnetic fields and also without a cutoff ($c \to \infty$), Eq. (4) becomes the well-known Aslamazov–Larkin result[41]. In the case that $H//c$, T_c and $\mu_0 H^c_{c2}(0)$ were estimated to be 20.9 K and, respectively 55 T (i.e., $\xi_{ab}(0) = 2.4$ nm) from the raw $\rho(T)$ curves by using a ~50% criterion, values consistent with the ones resulting from the UD scaling shown in Fig. 2. By using in Eq. (4) these T_c and $H^c_{c2}(0)$ values and $\xi_c(0) = 0.8$ nm, a rather good agreement is obtained with the experimental data except for the lowest fields (0 and 1 T, not represented in the figure). As commented above this may be due

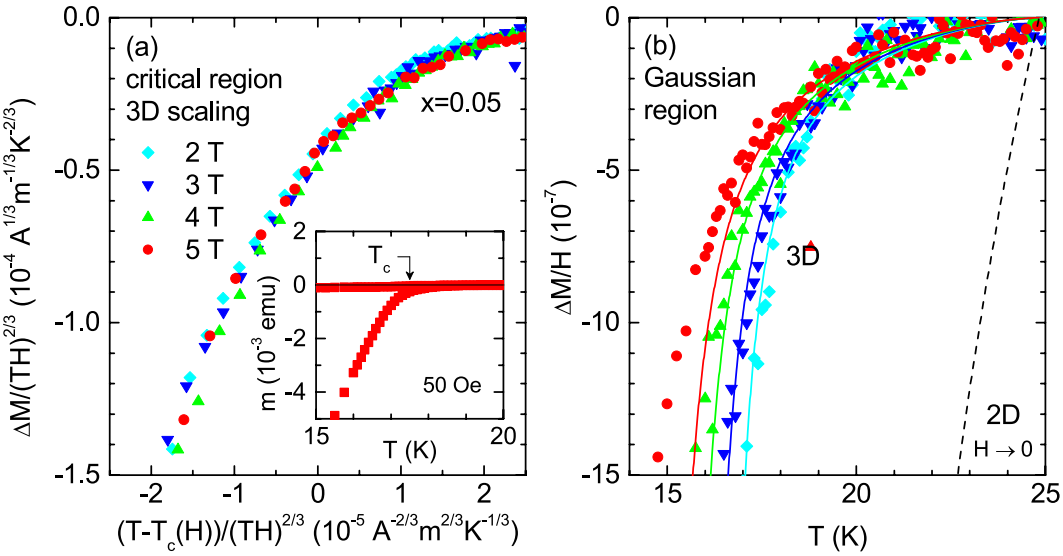

Figure 5. Analysis of the fluctuation magnetization (measured with $H//c$) for the $NaFe_{1-x}Co_xAs$ ($x = 0.05$) crystal. (**a**) 3D-UD scaling in the critical region, obtained by using $T_c = 17.5$ K and $B_{c2}(0) = 30$ T. (**b**) Temperature dependence of the fluctuation magnetic susceptibility in the Gaussian region. The solid lines correspond to the GL approach for 3D-anisotropic superconductors (Eq. 3), evaluated with the same T_c and $B_{c2}(0)$ values, and with $\gamma = 1.75$. For comparison, the prediction of the 2D approach is also shown as a dashed line (see the main text for details).

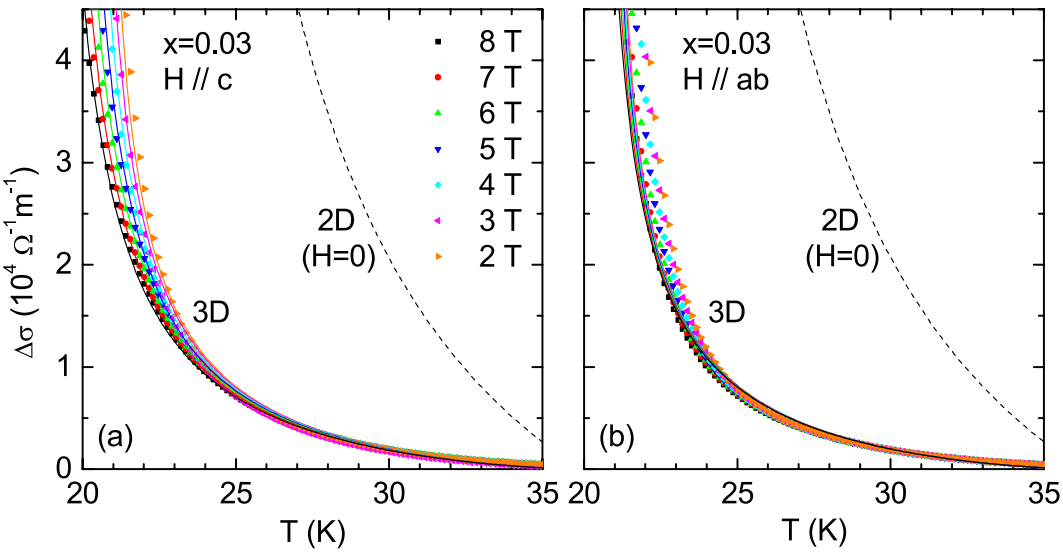

Figure 6. Temperature dependence of the fluctuation conductivity in the Gaussian region for the $NaFe_{1-x}Co_xAs$ ($x = 0.03$) crystal, for both $H//c$ (**a**) and $H//ab$ (**b**) under magnetic fields up to 8 T. The solid lines correspond to the Ginzburg-Landau approach for 3D-anisotropic superconductors, Eq. (4). For comparison, the prediction of the 2D approach is also shown as a dashed line (see the main text for details).

to a possible T_c distribution, although phase fluctuations and the multiband nature of these materials may also play a role[15,19,26,40]. The anisotropy factor resulted to be $\gamma = \xi_{ab}(0)/\xi_{ab}(0) \sim 3$. In case that $H//ab$, a relative good agreement was obtained without any free parameter by using a parallel upper critical field of $\mu_0 H_{c2}^{ab}(0) = \gamma \mu_0 H_{c2}^{c}(0) = 16$ T and to be consistent, the same values of T_c and $\xi_c(0)$. The agreement is not good near T_c and under the lowest fields, probably because the large $\mu_0 H_{c2}^{ab}(0)$ value extends the region affected by possible T_c distribution up to higher temperatures under the same applied fields (e.g., up to ~1 K above T_c under a 2 T field parallel to the ab layers). Again, just for completeness, the prediction of the 2D approach for $H = 0$ (that may be obtained from Eq. (4) in ref.[20] after setting $r = 0$, and that does not depend on any free parameter) is also included. Also in this case it strongly overestimates the observed $\Delta\sigma$.

In the case of the overdoped ($x = 0.073$) crystal, we failed to apply the 3D-GL approach for finite fields that was successfully applied in the case of optimal doped and lightly overdoped samples. As the comparison with the UD

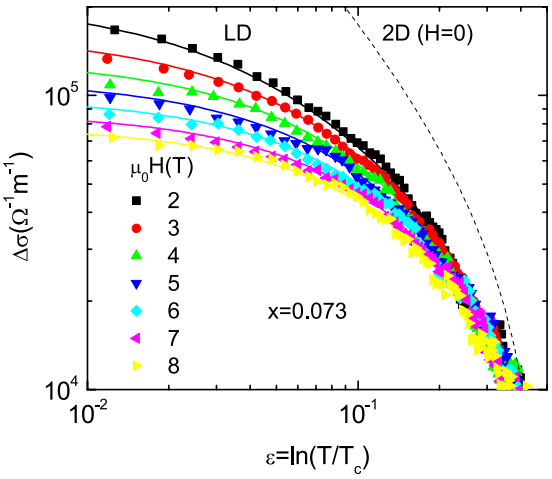

Figure 7. Temperature dependence of the fluctuation conductivity in the Gaussian region for the $NaFe_{1-x}Co_xAs$ ($x = 0.073$) crystal for magnetic fields up to 8 T perpendicular to the *ab* layers. The lines correspond to the Lawrence-Doniach approach for finite applied magnetic fields and under a total-energy cutoff (Eq. 5). For comparison, the prediction of the 2D approach is also shown as a dashed line (see the main text for details).

approach in the critical region suggests a dimensional transition in highly overdoped crystals, we will now probe a quasi-2DLawrence-Doniach (LD) approach for the in-plane fluctuation conductivity valid in presence of finite applied magnetic fields[20]. For magnetic fields perpendicular to the *ab* layers it reads

$$\Delta\sigma_{LD}(\varepsilon, h) = \frac{e^2}{64\pi\hbar}\frac{1}{h}\int_{-\pi/s}^{\pi/s} dk_z\left[\psi'\left(\frac{\epsilon + h + \omega_{kz}^{LD}}{2h}\right) + \psi'\left(\frac{c + h + \omega_{kz}^{LD}}{2h}\right)\right], \tag{5}$$

where ψ' is the polygamma function, $\omega_{kz}^{LD} = B_{LD}[1 - \cos(k_z S)]/2$, $B_{LD} = [2\xi_c(0)/s]^2$ is so called Lawrence-Doniach parameter, S is the interlayer distance, and c is the total-energy cutoff constant that corresponds to ε-value at which $\Delta\sigma$ vanishes. To compare with the experimental data, we used $T_c = 16.3$ K (as determined from the analysis of the critical region), $c = 0.5$ (according to the ε-value at which at which fluctuation effects vanish), and $s = 0.74$ nm[42]. As it is shown in Fig. 7, an excellent agreement was found by using for the remaining parameters $\xi_c(0) = 0.23$ nm and $\xi_{ab}(0) = 3.36$ nm. The $\xi_{ab}(0)$ value is close to the one determined from the analysis in the critical region (2.85 nm) which is a consistency check of our analysis. On the other hand, $\xi_c(0)$ is significantly smaller than the interlayer distance, which justifies the breakdown of the 3D-anisotropic GL approach and the need to use a LD approach. A similar $\xi_c(0)$ value is also found in optimally doped $YBa_2Cu_3O_x$ (also presenting a quasi-2D behavior on increasing the temperature above T_c), and in highly anisotropic pnictides like $Ca_{1-x}La_xFe_{1-y}Ni_yAs_2$[20], and overdoped $BaFe_{2-x}Ni_xAs_2$[18]. The $\xi_c(0)$ value reported in ref.[40] (1.43 nm) is significantly larger. However, in that work $H_{c2}(T)$ was estimated from the shift of resistive transition, a procedure that is highly dependent on the criterion used and that leads to a large uncertainty in the $H_{c2}(0)$ value, mainly when $H//ab$. As for the x = 0.05 and 0.03 crystals, the 2D approach (dashed line) strongly overestimates the observed $\Delta\sigma$ amplitude.

The superconducting parameters obtained in the above analysis are listed in Table 1, and represented against the doping level in Fig. 8. The anisotropy factor γ in our samples presents a strong dependence on the Co-doping level. While in the optimally-doped sample ($x = 0.03$) γ is estimated to be ~3.6, it is as large as 14.6 in the heavily overdoped sample (it is worth noting that in the slightly overdoped sample ($x = 0.05$) it was found $\gamma = 1.75$, a value still close to the one found in the optimally-doped compound. However, this result comes from measurements of the fluctuation magnetization, whose amplitude (that is directly proportional to γ) may be reduced by an incomplete superconducting volume fraction. This value is even larger than the one observed in 1111 compounds ($\gamma(T_c) \approx 6$–9)[6,43–45], and comparable to the one observed in crystals of $(Li_{1-x}Fe_xOH)FeSe$ and $Li_x(NH_3)_yFe_2Se_2$, for which $\gamma(T_c) \approx 15$[46,47]. The γ increase comes essentially from a significant reduction with the doping level of the transverse coherence length (that changes from ~0.8 nm for $x = 0.03$ to ~0.23 nm for $x = 0.07$), while $\xi_{ab}(0)$ remains almost constant (it only changes from ~2.4 nm to ~3.3 nm). The same effect was also observed in $Ba(Fe_{1-x}Ni_x)_2As_2$[26], for which $\gamma \sim 16$ was found when $x = 0.01$ (i.e. twice the optimal doping level, as in our present work). In the framework of the LD model $\xi_c(0)$ is related to the Josephson coupling constant Γ between adjacent superconducting layers through $\xi_c(0) = s\Gamma^{1/2}$[48,49]. Thus, our results seem to suggest that the FeAs-layers coupling may be significantly weakened by the Co doping.

Conclusions

We studied the fluctuation effects on the magnetotransport and the magnetization of $NaFe_{1-x}Co_xAs$ ($x = 0.03$, 0.05, 0.07, 0.073) single crystals. The data were compared with the Ullah & Dorsey (UD) scaling approach in the critical region around the $T_c(H)$ line, and the 3D-GL and quasi-2D LD approaches in the Gaussian region

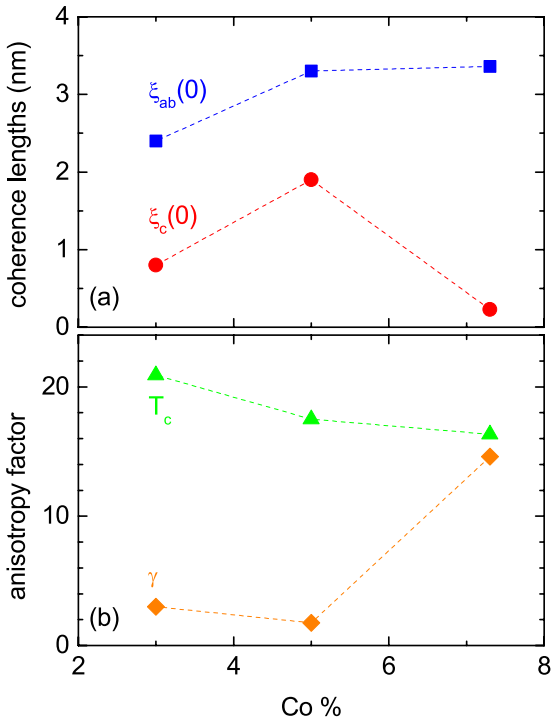

Figure 8. Doping-level dependence of the superconducting parameters, as result from the analysis of the fluctuation effects in the Gaussian region.

well above T_c. The analysis allowed to obtain the dependence with the doping level of fundamental parameters like the coherence lengths and the anisotropy, as well as of the effective dimensionality. While optimally-doped compounds present a moderate anisotropy and a three-dimensional behavior in the critical as well as in Gaussian region, the strongly overdoped compounds are among the most anisotropic iron pnictides, and present 3D characteristics only around $T_c(H)$, and follow quasi-2D approach well above T_c. Our results could be attributed to a weakening of the Josephson coupling between adjacent superconducting FeAs layers, induced by the Co-doping.

Methods

$NaFe_{1-x}Co_xAs$ ($x = 0.03, 0.05, 0.07, 0.073$) single crystals were grown by using the Bridgman method[22], by using Na chips, Co chips and FeAs precursors were used as starting materials. The FeAs precursor was synthesized by heating a mixture of Fe and As pieces in an evacuated quartz tube at 500 °C for 48 h, and then heating at 1000 °C for 48 h. In the final step, Na chips, Co chips, and FeAs precursor were mixed in the ratio Na:Fe:Co:As = 2:1-*x*:*x*:1.18 where $x = 0.03, 0.05, 0.07, 0.073$. The mixture for each specific ratio was put in a BN crucible which was in turn put in a W-crucible arc-welded in Ar-atmosphere. Finally, the W-crucible was heated at 1300 °C for about 6 h, followed by a slow downward movement at a rate of 2 mm/h in a vertical Bridgman furnace. After completion of heat treatment, typical dimensions of as-grown single crystals are $0.1 \times 1 \times 2\,mm^3$ for almost each of the three series of samples. We used single crystals from the same batches used in our recent paper[42]. During this study, XRD analyses revealed well defined (0 0 *l*) peaks with FWHM of about 0.05°. Furthermore, SEM images and EDS spectrum revealed that Na, Fe, Co and As are homogeneously distributed. We also performed HR-TEM analysis with FFT images, SAED patterns and theoretical spot diffraction. SAED pattern showed spots only along the zone axis [1 0 0] indicating good crystallinity of the samples. However, some stripes were found because of planar defects. However, at small scale FFT image didn't reveal any planar defects which indicate, as reported earlier[50], that these defects may occur due to dual beam FIB and by an intrinsic real structural defect due to Co doping. The in-plane resistivity was measured in the presence of magnetic fields up to 8 T perpendicular and along the crystal's ab-planes by using a Quantum Design's Physical Property Measurement System (PPMS). Electrical contacts of ~1 Ω were prepared by attaching gold wires to the crystals with silver paste in a glove box. The temperature dependence of the magnetization was measured with a commercial SQUID magnetometer (MPMS, Quantum Design). These measurements were performed in both zero-field-cooled (ZFC) and field cooled (FC) modes, with magnetic fields up to 50 kOe.

References

1. Tinkham, M. Introduction to Superconductivity (NewYork: McGraw-Hill), 2nded, ch8 (1996).
2. Ullah, S. & Dorsey, A. T. Critical Fluctuations in High-Temperature Superconductors and the Ettingshausen Effect. *Phys. Rev. Lett.* **65**, 2066 (1990).
3. Ullah, S. & Dorsey, A. T. Effect of fluctuations on the transport properties of type-II superconductors in a magnetic field. *Phys. Rev. B* **44**, 262 (1991).

4. Tesanovic, Z., Xing, L., Bulaevskii, L., Li, Q. & Suenaga, M. Critical Fluctuations in the Thermodynamics of Quasi-Two-Dimensional Type-II Superconductors. *Phys. Rev. Lett.* **69**, 3563 (1992).
5. Welp, U. *et al*. High-field scaling behavior of thermodynamic and transport quantities of $YBa_2Cu_3O_{7-\delta}$ near the superconducting transition. *Phys. Rev. Lett.* **67**, 3180 (1991).
6. Welp, U. *et al*. Anisotropic phase diagram and superconducting fluctuations of single-crystalline $SmFeAsO_{0.85}F_{0.15}$. *Phys. Rev. B* **83**, 100513(R) (2011).
7. Pallecchi, I. *et al*. Upper critical field and fluctuation conductivity in the critical regime of doped SmFeAsO. *Phys. Rev. B.* **79**, 104515 (2009).
8. Kim, S. H. *et al*. Fluctuation conductivity of single-crystalline $BaFe_{1.8}Co_{0.2}As_2$ in the critical region. *J. Appl. Phys.* **108**, 063916 (2010).
9. Wang, A. F. *et al*. Phase diagram and calorimetric properties of $NaFe_{1-x}CoxAs$. *Phys. Rev. B.* **85**, 224521 (2012).
10. JianqiangHou, Philipp Burger, Huen Kit Mak, Frédéric Hardy, Thomas Wolf, Christoph Meingast, and Rolf Lortz, Doping dependence of the critical fluctuation regime in the Fe-based superconductor $Ba_{1-x}K_xFe_2As_2$, Phys. Rev. B **92**, 064502 (2015).
11. Yang, H., Chen, G., Zhu, X., Xing, J. & Wen, H.-H. BCS-like critical fluctuations with limited overlap of Cooper pairs in FeSe. *Phys. Rev. B* **96**, 064501 (2017).
12. Choi, C. *et al*. The fluctuation effect of $BaFe_{1.8}Co_{0.2}As_2$ single crystals from reversible magnetization. *Supercond. Sci. Technol.* **22**, 105016 (2009).
13. Salem-Sugui, S. *et al*. Superconducting fluctuations in the reversible magnetization of the iron- pnictide $Ba_{1-x}K_xFe_2As_2$. *Phys. Rev. B.* **80**, 014518 (2009).
14. Mosqueira, J. *et al*. Observation of anisotropic diamagnetism above the superconducting transition in iron pnictide $Ba_{1-x}K_xFe_2As_2$ single crystals due to thermodynamic fluctuations. *Phys. Rev. B.* **83**, 094519 (2011).
15. Prando, G. *et al*. Superconducting phase fluctuations in $SmFeAsO_{0.8}F_{0.2}$from diamagnetism at a low magnetic field above. *Tc. Phys. Rev. B.* **84**, 064507 (2011).
16. Ahmad, D. *et al*. Vortex fluctuation effect evaluated using reversible magnetization in optimally doped single crystal $NaFe_{0.97}Co_{0.03}As$. *Supercond. Sci. Technol.* **27**, 125006 (2014).
17. Bossoni, L., Romanó, L., Canfield, P. C. & Lascialfari, A. Non-conventional superconducting fluctuations in $Ba(Fe_{1-x}Rh_x)_2As_2$ iron-based superconductors. *J. Phys.: Condens. Matter* **26**, 405703 (2014).
18. Ramos-Álvarez, A., Mosqueira, J., Vidal, F., Lu, Xingye. & Luo, Huiqian. Large increase of the anisotropy factor in the overdoped region of $Ba(Fe_{1-x}Ni_x)_2As_2$ as probed by fluctuation spectroscopy. *Supercond.Sci. Technol.* **28**, 075004 (2015).
19. Ramos-Álvarez, A. *et al*. Superconducting fluctuations in isovalently substituted $BaFe_2(As_{1-x}P_x)_2$: Possible observation of multiband effects. *Phys. Rev. B.* **92**, 094508 (2015).
20. Sóñora., D. *et al*. Quasi-two-dimensional behavior of 112-type iron-based superconductors. *Phys. Rev. B.* **96**, 014516 (2017).
21. Fanfarillo, L., Benfatto, L., Caprara, S., Castellani, C. & Grilli, M. Theory of fluctuation conductivity from interband pairing in pnictide superconductors. *Phys. Rev. B.* **79**, 172508 (2009).
22. Putti, M. M. *et al*. New Fe-based superconductors: properties relevant for applications. *Supercond. Sci. Technol.* **23**, 034003 (2010).
23. Song, Y. J., Kang, B., Rhee, J. S. & Kwon, Y. S. *Thermally activated flux flow and fluctuation conductivityin LiFeAs single crystalEurophys. Lett.* **97**, 47003 (2012).
24. Rullier-Albenque, F., Colson, D., Forget, A. & Alloul, H. Multiorbital Effects on the Transport and the Superconducting Fluctuations in LiFeAs. *Phys. Rev. Lett.* **109**, 187005 (2012).
25. Marra, P. *et al*. Paraconductivity of the K-doped $SrFe_2As_2$ superconductor. *New J. Phys.* **14**, 043001 (2012).
26. Rey, R. I. *et al*. Measurements of the fluctuation-induced in-plane magnetoconductivity at high reduced temperatures and magnetic fields in the iron arsenide $BaFe_{2-x}Ni_xAs_2$. *Supercond. Sci. Technol.* **26**, 055004 (2013).
27. Rey, R. I. *et al*. Measurements of the superconducting fluctuations in optimally doped $BaFe_{2-x}Ni_xAs_2$ under high magnetic fields: probing the 3D-anisotropic Ginzburg-Landau approach. *Supercond. Sci. Technol.* **27**, 075001 (2014).
28. Ahmad, D., Seo, Y. I., Choi, W. J. & Kwon, Y. S. Effect of proton irradiation on the fluctuation-induced magnetoconductivity of $FeSe_{1-x}Te_x$ thin films. *New J. Phys.* **19**, 093004 (2017).
29. Ahmad, D., Seo, Y. I. & Choi, W. J. and Yong Seung Kwon, Fluctuation-induced magnetoconductivity in pristine and proton-irradiated $Ca_{8.5}La_{1.5}(Pt_3As_8)(Fe_2As_2)_5$ single crystals. *Supercond. Sci. Technol.* **30**, 025009 (2017).
30. Nabeshima, F., Nagasawa, K., Maeda, A. & Imai, Y. Superconducting fluctuations in $FeSe_{0.5}Te_{0.5}$ thin films probed via microwave spectroscopy. *Phys. Rev. B* **97**, 024504 (2018).
31. Ausloos, M. & A. A. Varlamov, A. A. Fluctuation Phenomena in High Temperature Superconductors, edited by (Springer, 1997).
32. Ramos-Álvarez, A., Mosqueira, J. & Vidal, F. Comment on Multiorbital Effects on the Transport and the Superconducting Fluctuations in LiFeAs. *Phys. Rev. Lett.* **115**, 139701 (2015).
33. Dinah, R. P. *et al*. Control of the Competition between a Magnetic Phase and a Superconducting Phase in Cobalt-Doped and Nickel-Doped NaFeAs Using Electron Count. *Phys. Rev. Lett.* **104**, 057007 (2010).
34. Ohashi, T., Kitano, H., Tsukada, I. & Maeda, A. ritical charge dynamics of superconducting $La_{2-x}Sr_xCuO_4$ thin films probed by complex microwave spectroscopy: Anomalous changes of the universality class by hole doping. *Phy. Rev. B.* **79**, 184507 (2009).
35. Zaanen, J. Specific-heat jump at the superconducting transition and the quantum critical nature of the normal state of pnictide superconductors. *Phy. Rev. B.* **80**, 212505 (2009).
36. Roulin, M., Junod, A. & Walker, E. Scaling behavior of the derivatives of the specific heat of $YBa_2Cu_3O_{6.93}$ at the superconducting transition up to 16 tesla. *Physica C.* **260**, 257 (1996).
37. Soto, F. *et al*. In-plane and transverse superconducting fluctuation diamagnetism in the presence of charge-density waves in 2H−$NbSe_2$ single crystals. *Phy. Rev. B.* **75**, 094509 (2007).
38. Vidal, F. *et al*. On the consequences of the uncertainty principle on the superconducting fluctuationswell inside the normal state. *Europhys. Lett.* **59**, 754 (2002).
39. Adachi, K. & Ikeda, R. Fluctuation diamagnetism in two-band superconductors. *Phys. Rev. B.* **93**, 134503 (2016).
40. Koshelev, A. E. & Varlamov, A. A. Fluctuations in two-band superconductors in strong magnetic field. *Supercond. Sci. Technol.* **27**, 124001 (2014).
41. Aslamazov, L. G. & Larkin, A. I. The influence of fluctuation pairing of electrons on the conductivity of normal metal. *Phys. Lett. A.* **26**, 238 (1968).
42. Choi, W. J., Seo, Y. I., Ahmad, D. & Kwon, Y. S. Thermal activation energy of 3D vortex matter in $NaFe_{1-x}Co_xAs$ ($x = 0.01$, 0.03 and 0.07) single crystals. *Sci. Rep.* **7**, 10900 (2017).
43. Jaroszynski, J. *et al*. Upper critical fields and thermally-activated transport of $NdFeAsO_{0.7}F_{0.3}$ single crystal. *Phys. Rev. B.* **78**, 174523 (2008).
44. Lee, H. S. *et al*. Effects of two gaps and paramagnetic pair breaking on the upper critical field of $SmFeAsO_{0.85}$ and $SmFeAsO_{0.8}F_{0.2}$ single crystals. *Phys. Rev. B.* **80**, 144512 (2009).
45. Karpinski, J. *et al*. Single crystals of $LnFeAsO_{1-x}F_x$ (Ln = La, Pr, Nd, Sm, Gd) and $Ba_{1-x}Rb_xFe_2As_2$. *Physica C.* **469**, 370 (2009).
46. Xiaolei, Y. *et al*. Vortex phase transition and anisotropy behavior of optimized $(Li_{1-x}Fe_xOH)FeSe$ single crystals. *Supercond. Sci. Technol.* **29**, 105015 (2016).
47. Sun, S., Wang, S., Yu, R. & Hechang, L. Extreme anisotropy andAnomalous transport properties of heavily electron doped $Li_x(NH_3)_yFe_2Se_2$ single crystals. *Phys. Rev. B.* **96**, 064512 (2017).
48. Klemm, R. A., Luther, A. & Beasley, M. R. Theory of the upper critical field in layered superconductor. *Phys. Rev. B.* **12**, 877 (1975).

49. Ramallo, M. V., A. Pomar, A. & Vidal, F. In-plane paraconductivity and fluctuation-induced magnetoconductivity in biperiodic layered superconductors: Application to $YBa_2Cu_3O_{7-\delta}$. *Phys. Rev. B.* **54**, 4341 (1996).
50. Friederichs, G. M. *et al.* Metastable 11 K superconductor $Na_{1-y}Fe_{2-x}As_2$. *Inorg. Chem.* **51**, 8161 (2012).

Acknowledgements

YSK was supported by the NRF grant funded by the Ministry of Science, ICT and Future Planning (2015M2B2A9028507, 2016R1A2B4012672). DA and YSO was partially supported by the National Research Foundation of Korea (NRF) grant funded by the Korea government (MSIT) (NRF-2017R1A4A1015323). DS and JM acknowledge financial support from Project No. FIS2016-79109-P (AEI/FEDER, UE). TP was supported by the NRF grant funded by the Ministry of Science, ICT and Future Planning of Korea (No. 2012R1A3A2048816). YSO was supported by the National Research Foundation of Korea (NRF) grant funded by the Korea government (MSIT) (NRF-2015R1C1A1A01055964).

Author Contributions

D.A., W.J.C. and Y.C.K. performed magnetization and magnetotransport measurements. D.A. and W.J.C. prepared and characterized single crystalline samples. D.A., J.M. and D.S. did data analysis. D.A., Y.S.K. and J.M. wrote the manuscript. Y.S. Oh. and T.P. also helped in data analysis. All authors discussed the results and reviewed the manuscript.

Additional Information

Competing Interests: The authors declare no competing interests.

Publisher's note: Springer Nature remains neutral with regard to jurisdictional claims in published maps and institutional affiliations.